Complex Processing–Morphology Interrelationships During the Reactive Compatibilization of Blends of Poly(butylene terephthalate) with Epoxide-Containing Rubber

P. Martin,[1] J. Devaux,[1] R. Legras,[1] L. Leemans,[2] M. van Gurp,[2] M. van Duin[2]

[1]*Laboratoire des Hauts Polymères, Université Catholique de Louvain, 1, Place Croix du Sud, 1348 Louvain-la-Neuve, Belgium*
[2]*DSM Research, P.O. Box 18, 6160 MD Geleen, The Netherlands*

Received 26 November 2002; accepted 4 May 2003

ABSTRACT: Reactive processing of blends of poly(butylene terephthalate) (PBT) with the ethene–(methyl acrylate)–(glycidyl methacrylate) terpolymer (E–MA–GMA) is known to present a very complex reactivity since two competitive reactions take place spontaneously during melt blending, that is, blend compatibilization and rubber-phase crosslinking. In this article, the effects of several processing parameters, such as the shear rate, the processing temperature, and the matrix viscosity, on the reactive processing of those blends were investigated in terms of the blend morphology and of the amount of copolymer formed at the blend interface. It was shown that the morphology development could be divided in two successive regimes: In the early stages of the mixing process, the particle size is essentially determined by the physical dispersion process, that is, breakup and coalescence, while, at longer mixing times, a further decrease in particle size is obtained as a result of the compatibilization reactions. The shift between the two regimes is progressive and intimately related to the processing conditions. Despite such a complexity, not only the blend morphology but also the elastic properties of the rubber particles can be controlled in a broad range by an adequate adjustment of the relative kinetics between both physical and chemical processes. © 2003 Wiley Periodicals, Inc. J Appl Polym Sci 91: 703–718, 2004

Key words: compatibilization; crosslinking; processing; morphology

INTRODUCTION

Polyesters, such as poly(butylene terephthalate) (PBT) or poly(ethylene terephthalate (PET), generally exhibit high stiffness, good thermal aging resistance, and excellent dimensional stability. These polymers provide very useful material for automotive and electronic applications.[1] Unfortunately, polyesters are also notch-sensitive, brittle, and sensitive to the hydrolysis. Thus, there is an interest in developing compatible polyester/rubber blends. Such blends have attracted much attention over the last decade.[2–21] To obtain improved impact resistance, a good dispersion of the rubber is required. Blend compatibilization is, therefore, indispensable.

Reactive compatibilization of polyester/polyolefin blends can be achieved by several approaches based on the reactivity of the carboxyl and the hydroxyl end groups of the polyesters. In this context, acrylate-based copolymers,[2–4] maleic anhydride-containing elastomers,[5–7] epoxidized polyolefins,[8–18] the ethylene–vinyl acetate copolymer,[19] an oxazoline-modified polymer,[20] and core–shell impact modifiers[21] have already been used as toughening agents. In most cases, epoxide-containing rubbers appeared to be the most effective to toughen both PBT and PET. Such elastomers promote, indeed, the finest morphology, the greatest interfacial adhesion, and, subsequently, the best mechanical properties.[14–18]

Blends of polyesters with epoxide-containing rubbers exhibit, however, a very complex reactivity. In a recent study on the compatibilization of PBT with the terpolymer of ethylene (E), methylacrylate (MA), and glycidyl methacrylate (GMA), we demonstrated that two competitive reactions take place simultaneously during melt processing, namely: (i) compatibilization as a result of interfacial reactions between carboxyl PBT chain ends and terpolymer epoxide groups, resulting in the formation of E–MA–GMA/PBT graft copolymers, and (ii) rapid crosslinking of the rubber phase as a result of the consequent reaction between epoxide groups on E–MA–GMA chains triggered by the formed hydroxyl groups.[22] The competition between compatibilization and crosslinking was shown to be dependent on the type of terpolymer, that is,

Correspondence to: P. Martin (martin@poly.ucl.ac.be).
Contract grant sponsor: DSM.

TABLE I
Characteristics of the Different PBT Grades

PBT grade	[—COOH] (μequiv/g)	[—COOH] (μequiv/g)	Relative viscosity η_r in *m*-cresol	M_n (kg/mol)
L-PBT	45	66	1.85	16.1
M-PBT	49	31	2	19.8
H-PBT	42	10	2.4	30.9

virgin E–MA–GMA or a modified terpolymer rubber. This latter rubber grade was prepared by melt mixing pure E–MA–GMA with a calculated amount of low molecular weight acid in order to modify part of the epoxide groups. Two different blending mechanisms with polyesters were distinguished depending on whether pure or modified E–MA–GMA was used.[23] In the case of the modified terpolymer, secondary hydroxyl groups are present in the rubber phase from the beginning due to the modification step. When blending with PBT, a true competition between compatibilization of the blend and crosslinking of the rubber phase takes place in the melt. Crosslinking proceeds homogeneously throughout all the E–MA–GMA particles, which affects both dispersion and coalescence processes. For PBT blends with an unmodified terpolymer, competition between the two types of reactions is somewhat delayed. In the first stages of mixing, graft copolymers are formed, which generates secondary —OH groups on the rubber chains close to the interphase. Subsequently, crosslinking starts and proceeds from the interface to the core of the dispersed-phase particles. The morphology development is thus more complex and the dispersed-phase particles will probably have a large heterogeneity and may even have a core–shell-type structure. All these phenomena result in very complex processing/morphology interrelationships and affect also the final blend properties.

This article addresses the question of the possibility to control such complex phenomena to obtain tailored blend morphologies and, consequently, improved final properties. For this purpose, the effects of various processing parameters such as the screw speed, the temperature, the phase reactivity, as well as the matrix viscosity on both blend compatibilization and rubber phase crosslinking were investigated. The results showed that independent modulation of the blend morphology and of the elastic properties of the rubber particles can be achieved by an adequate choice of the processing conditions. These conclusions can be extended to any polymer blend containing epoxide-functionalized polymers.

EXPERIMENTAL

Materials

Three PBT grades of different molecular weights were supplied by DSM (Geleen, The Netherlands). Their main characteristics, such as acid and hydroxyl chain end concentration and relative viscosity, are given in Table I. Each PBT grade is identified by its molecular weight (H: high, M: medium, and L: low). Lotader AX8900 (E–MA–GMA) was purchased from the Elf–Atochem Co. (Saint-Avold, France). The composition is 68 wt % E, 24 wt % MA, and 8 wt % GMA according to the manufacturer. Some small deviation from the prospect data can be expected in some cases as reported by Papke and Karger-Kocsis[24] The melt-flow index is 6 g/10 min at 190°C under 2.16 kg. Its number-average and weight-average molecular weights are 10 and 31 kg/mol, respectively. According to these values, one can calculate the average number of epoxide functions per terpolymer chain, which, in this case, is equal to five to six functions per chain. Lotril 28MA07 (E–MA) was also purchased from the Elf–Atochem Co. and is rather similar to Lotader AX8900, namely, a composition of 30 wt % MA content and an MFI of 6 g/10 min at 190°C under 2.16 kg. Despite some differences in the chemical structure, dynamic mechanical thermal analysis (DMTA) and cloud-point experiments demonstrated that E–MA–GMA and E–MA are fully miscible.

Forty-eight weight percent-modified E–MA–GMA was synthesized in the melt by mixing E–MA–GMA with a calculated amount of *para-t*-butylbenzoic acid molecules according to the procedure previously described.[22] *Para-t*-butylbenzoic acid and solvents were purchased from the ACROS Chemical Co. (Geel, Belgium) and were used as received.

Processing

Prior to processing, all materials were dried overnight at 25°C under a vacuum. Although standard PBT drying conditions are 125°C under a vacuum, preliminary experiments comparing both drying conditions have not shown any effect on PBT degradation and on the compatibilization process for the experiments performed in the internal mixer.[22]

PBT/rubber blends were prepared using a Brabender WE 50H internal mixer. The atmosphere in the mixer was controlled by purging with nitrogen gas. Blend compositions were 80/20 (w/w) PBT/rubber, except when specified differently. The PBT pellets were molted for 1 min at 30 rpm prior to addition of the rubber powder. Immediately after introduction of

TABLE II
Processing Conditions for the Different PBT/Rubber Blends

Matrix	Rubber phase	Temperature (°C)	Screw speed (rpm)
L-PBT	E–MA	250	90
	E–MA–GMA	250	90
M-PBT	E–MA	250	50
		250	90
		280	90
	E–MA–GMA	250	50
		250	90
		280	90
	48% modified E–MA–GMA	250	50
		250	90
		280	90
H-PBT	E–MA	250	90
	E–MA–GMA	250	90

the rubber powder, the rotation speed was increased to the final required value. The zero time was taken when all the rubber was introduced and the total mixing time was fixed at 18 min. At different times after rubber addition, samples were rapidly withdrawn from the mixing cavity and quenched in liquid nitrogen to stop the interfacial reactions and freeze in the morphology. Table II presents the processing conditions for the different PBT/rubber blends performed in this study.

Fractionation

A procedure was developed for removing free PBT from the PBT/rubber blends. Approximately a 1 g blend was introduced in 30 mL of pure trifluoroacetic acid (TFA), a good selective solvent for PBT, and stirred at room temperature for 1 h to solubilize the PBT phase. A milky emulsion was obtained and ultracentrifugated at 14°C and 25,000 rpm using a Beckman L7-65 ultracentrifuge. After 1 h 45 min, clear separation was achieved. The grafted rubber particles were concentrated as a white layer at the top of the centrifugation tube. The clear TFA solution was carefully removed and the dissolved PBT was precipitated in methanol, filtrated over a 0.5 μm PTFE filter, washed with methanol, and dried at 30°C under a vacuum for 24 h to yield the fraction *P1*. The rubber phase was dispersed again in 30 mL TFA and stirred for 45 min at room temperature. A second ultracentrifugation was performed for 1 h 45 min at 8°C and 28,000 rpm. Once again, the TFA solution containing free PBT was carefully separated from the rubber phase, precipitated, and worked up to form the fraction *P2*. This fraction represents only approximately 3 wt % of the total amount of material. Complete recovery of nongrafted PBT was achieved after the second washing step, since no additional free PBT was obtained when a third separation was carried out. The total amount of free PBT is equal to the sum of fractions *P1* and *P2* and is noted as *P*.

After separation, the rubber phase was stirred in chloroform ($CHCl_3$) at 50°C for 1 h and filtrated. Hot $CHCl_3$ is a selective solvent for both E–MA and E–MA–GMA. An insoluble fraction, called *C*, was recovered. The free rubber was precipitated from the $CHCl_3$ solution in methanol, filtrated, and dried for 24 h at 30°C under a vacuum, yielding fraction *R*.

The weights of the initial sample and of the different fractions were precisely measured. Due to the large number of experimental steps, some material was lost. Still, the mass recovery was always above 90%. The amount of grafted PBT was estimated by comparison between the initial PBT content, which was equal to 80 wt % for all blends, and the PBT amount recovered in fractions *P1* and *P2*.

Each separation was performed on at least two blend samples. Different batches of modified E–MA–GMA were produced and used successively for blending with PBT leading to truly duplicate polymer blends. The reported results correspond to mean values of all these separations. The standard deviation for each blend fraction *P1*, *P2*, *R*, and *C* was, in all cases, below 15%. Besides the weight of each fraction, its composition was also quantitatively determined using Raman spectroscopy.

Spectroscopy

Raman spectra were recorded at 25°C on a Labram confocal laser Raman spectrometer from Dilor S.A. in the spectroscopic mode. The excitation wavelength was 632.8 cm^{-1} from a He—Ne laser source. The pinhole aperture and the entrance slit were both fixed to 1000 μm, which resulted in a large analyzed volume of samples. A grating of 1800 grooves/mm was used and the spectra were recorded on a CCD detector. Spectra were centered on 2900 cm^{-1}. Each spectrum was the average of five accumulations of 60 s. PBT and E–MA–GMA can be distinguished and separately quantified using the vibrational bands in the region of 2500–3250 cm^{-1}. A previously developed calibration curve was used.[22]

Microscopy

The blend morphology was examined by transmission electron microscopy (TEM). For this purpose, samples were ultramicrotomed in thin films of approximately 70–80 nm at −80°C to avoid deformation of the dispersed-phase particles. The microtomed cuts were stained for 6 min under RuO_4 vapor before examination with a Philips EM 301 microscope.

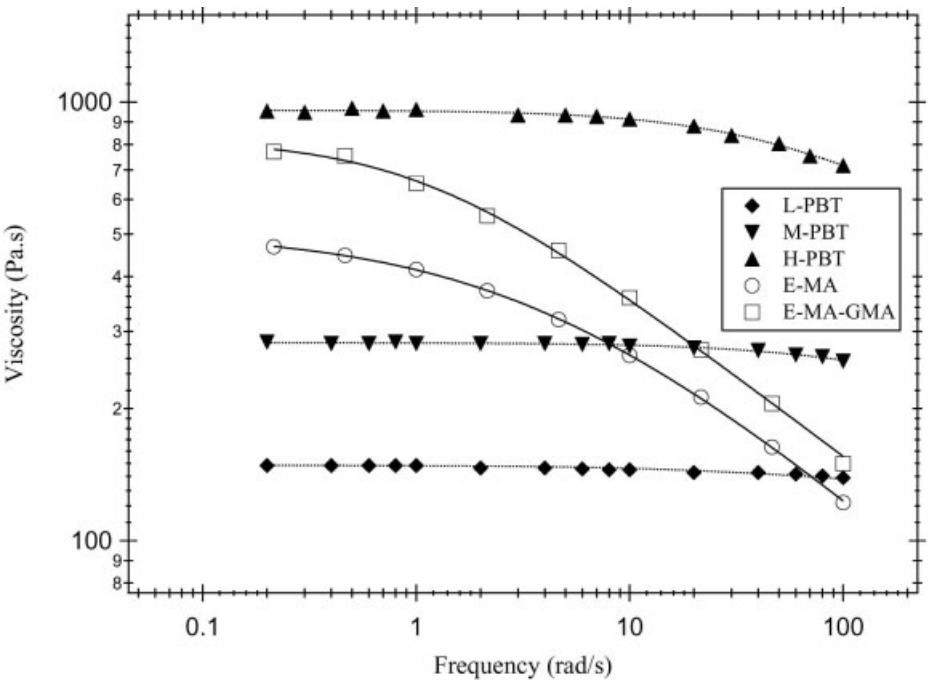

Figure 1 Shear viscosity versus frequency for the blend components at 250°C. The experimental points were fitted using a Carreau–Yasuda four-parameter model.

After examination, the morphology was quantified by image analysis. For each sample, at least 200 particles were measured by hand and both the volume and the number-average diameters, D_v and D_n, respectively, were estimated on a Macintosh computer using the public domain NIH Image program (developed at the U.S. National Institutes of Health).

Rheology

The rheological properties of the molten PBT and E–MA–GMA polymers were measured using a Rheometrics ARES strain-controlled rheometer equipped with a parallel-plate geometry with a diameter of 25 mm and a gap of about 1.5 mm. Frequency-sweep experiments were performed at 250 and 280°C under a nitrogen atmosphere. The frequency ranged from 0.1 to 100 rad/s. Care was taken to keep the experiment within the linear viscoelastic domain. For this purpose, the strain response was maintained below 5%.

Molau's test

The so-called Molau's test measures the stability of a dispersion. PBT/rubber (80/20, w/w) blends were dissolved in TFA, a selective solvent for PBT. Dissolution was performed under moderate stirring for 12 h. The solution was then left at rest for 2 days. If the milky aspect, because of the nonsoluble dispersed rubber particles in the emulsion, remains after this time, it is concluded that the dispersed phase is stabilized and that sufficient copolymer/compatibilizer is present. Otherwise, a white skin is formed on the top of the solution due to the coagulation of the nonstabilized rubber particles.

RESULTS

Rheological behavior of the blend components

Figures 1 and 2 present the evolution of the shear viscosity as a function of the frequency for the PBTs and the rubbers at 250 and 280°C. All PBT grades display a Newtonian behavior almost in the whole frequency range independent of the temperature. In contrast, the viscosities of both E–MA and E–MA–GMA exhibit Newtonian plateaus at low frequencies and elastic behaviors at high frequencies. These experimental data were fitted using a Carreau–Yasuda four-parameter model to determine the zero-shear viscosity η_0 of the components as well as to model their frequency dependence:

$$\eta = \eta_0[1 + (\lambda\dot{\gamma})^a]^{n-1/a} \quad (1)$$

where η is the shear viscosity; n, the power-law coefficient; λ, a characteristic time for the transition between the Newtonian and the shear-thinning regime, and a, a parameter related to the curvature of this transition. The values for the zero-shear viscosity are given for each component as a function of the temperature in Table III. It is clear that the higher the tem-

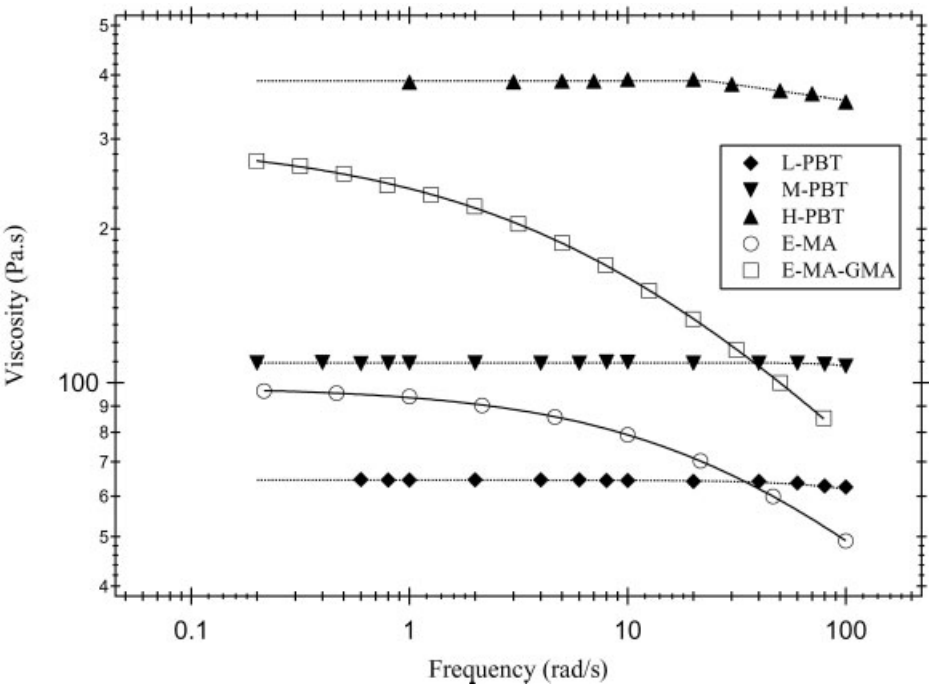

Figure 2 Shear viscosity versus frequency for the blend components at 280°C. The experimental points were fitted using a Carreau–Yasuda four-parameter model.

perature, the lower is the shear viscosity. The effect is more noticeable for the rubbers.

PBT/rubber blends

Effect of the rotation speed

Figure 3 presents the evolution of the number-average rubber particle diameter, D_n, as a function of the mixing time at 250°C for the M-PBT/E–MA (80/20, w/w) nonreactive blend at two different rotation speeds. It is clear that the higher the rotation speed, the finer is the final dispersion. After 18 min of mixing, D_n was equal to 1.40 and 0.75μm at 50 and 90 rpm, respectively.

TABLE III
Values of the Zero-shear Viscosity η_0 for the PBTs and the Rubbers at 250 and 280°C

Polymer	Temperature (°C)	η_0 (Pa s)
L-PBT	250	148.5
	280	64.5
M-PBT	250	282.5
	280	109.5
H-PBT	250	958
	280	389
E–MA–GMA	250	822.5
	280	298.5
E–MA	250	506
	280	98

Error bars refer to the standard deviation of the particle-size distribution. In both cases, the size of the rubber particles decreases as the mixing time increases and finally reaches a plateau at long mixing times, that is, typically longer than 6 min.

The influence of the shear rate on the morphology development was also investigated in the case of PBT/E–MA–GMA reactive blends. Figure 4(a,b) shows the evolution of the rubber particle size as a function of the mixing time at 250°C at 50 and 90 rpm, for M-PBT/E–MA–GMA and M-PBT/48 %-modified E–MA–GMA (80/20, w/w) blends, respectively. Whatever the nature of the rubber phase, the size of the dispersed-phase particles is significantly smaller than the values obtained for the nonreactive M-PBT/E–MA blends (Fig. 3). As shown in Figure 4(a,b), submicrometer dimensions are obtained very rapidly, even at the lowest rotation speed, that is, 50 rpm. Whatever the screw speed and the rubber phase, the blend morphology remains unchanged after approximately 3 min of mixing, namely, D_n reaches a plateau. These observations are in agreement with previous results[22] and can be related to the formation of the E–MA–GMA/PBT graft copolymer at the blend interface during processing. In agreement with the results for M-PBT/E–MA nonreactive blends, increasing the shear rate in the internal mixer from 50 to 90 rpm results in a finer dispersion from 0.28 to 0.18 μm for M-PBT/E–MA–GMA (80/20, w/w) blends. In the case of M-PBT/48%-modified E–MA–GMA blends, the effect

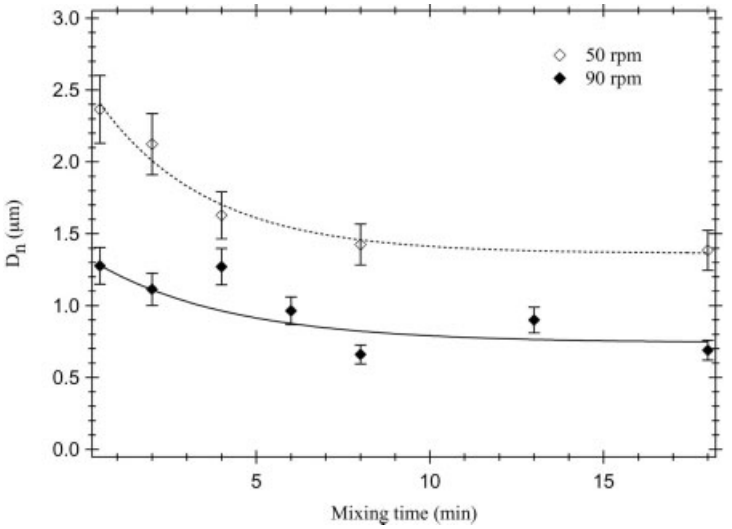

Figure 3 Effect of the screw speed on the evolution of dispersed particle size as a function of mixing time for M-PBT49/E–MA (80/20, w/w) blends at 250°C.

is even more noticeable since D_n decreases from 0.34 to 0.18 μm under the same conditions. It is worth noting that, at high shear rates, the final morphology appears to be independent of the used rubber, that is, pure or 48%-modified E–MA–GMA.

To obtain more insight in the chemical reactions occurring in the system for the different processing conditions, the amount of grafted PBT was quantified using the developed separation procedure. The evolution of the P (free PBT chains) and R (free rubber chains) fractions as a function of the mixing time and the processing conditions are presented in Figures 5 and 6, respectively. For the same processing conditions, M-PBT blends containing virgin E–MA–GMA contain a higher amount of PBT chains grafted to the rubber particles. However, whatever the rubber phase, the amount of grafted PBT chains (calculated as $80 - P$) is higher for experiments performed at 90 versus 50 rpm. More interesting is the evolution of the amount of free rubber, R, as a function of the mixing time (Fig. 6). In the case of M-PBT/48%-modified E–MA–GMA blends, the amount of free rubber after 8 min of mixing is very small and independent of the screw speed. In contrast, for M-PBT blends containing pure E–MA–GMA, R was found to be equal to 1.0 and 4.3% at 90 and 50 rpm, respectively. The amount of free rubber chains appears, therefore, to be inversely proportional to the screw speed.

At this stage, it is important to note that the amount of grafted PBT chains (calculated as $80 - P$) is not representative for the kinetics of the interfacial reaction, since this value depends also of the amount of interfacial area available for the coupling reaction. For a more thorough interpretation, the amount of grafted PBT has to be normalized to the corresponding available interfacial area. In other words, one has to calculate the average area A occupied by a copolymer chain at the blend interface.[25–27] Within the limits of the assumption that all the compatibilizer graft copolymers are and remain at the interface, Paul and Newman[28] proposed to express A by

$$A = \left(\frac{6}{D_n}\right)\phi_d \frac{M}{N_{\text{av}}W} \tag{2}$$

where M is the number-average molecular weight of the compatibilizer; W, its weight/volume content, N_{av}, the Avogadro number; D_n, the number-average diameter; and Φ, the volume fraction of the dispersed rubber phase. In the present study, M and W are unknown since the graft copolymer cannot be isolated and, therefore, characterized. As a rough approximation, the molecular weight of the original PBT and the amount of grafted PBT were used in eq. (2). M and W are thus underestimated, this error being compensated by the fact that A depends on the ratio of these parameters.[29] The value $1/A$ represents the interfacial copolymer concentration, that is, the number of PBT grafts per square nanometers of the interface.

The evolution of $1/A$ for the four PBT/E–MA–GMA reactive blends is presented in Figure 7. It is clear that M-PBT blends containing virgin E–MA–GMA have lower $1/A$ values than those of M-PBT/48%-modified E–MA–GMA blends. Whatever the used rubber phase, it is surprising to note that, after 8 min of mixing, the interfacial copolymer concentration $1/A$ is twofold higher at a low rotation speed (Table IV). In comparing Figures 4 and 7, one may conclude that an interfacial copolymer concentration of about 0.1 chain/nm^2 appears to be sufficient to promote stabilization of the morphology.

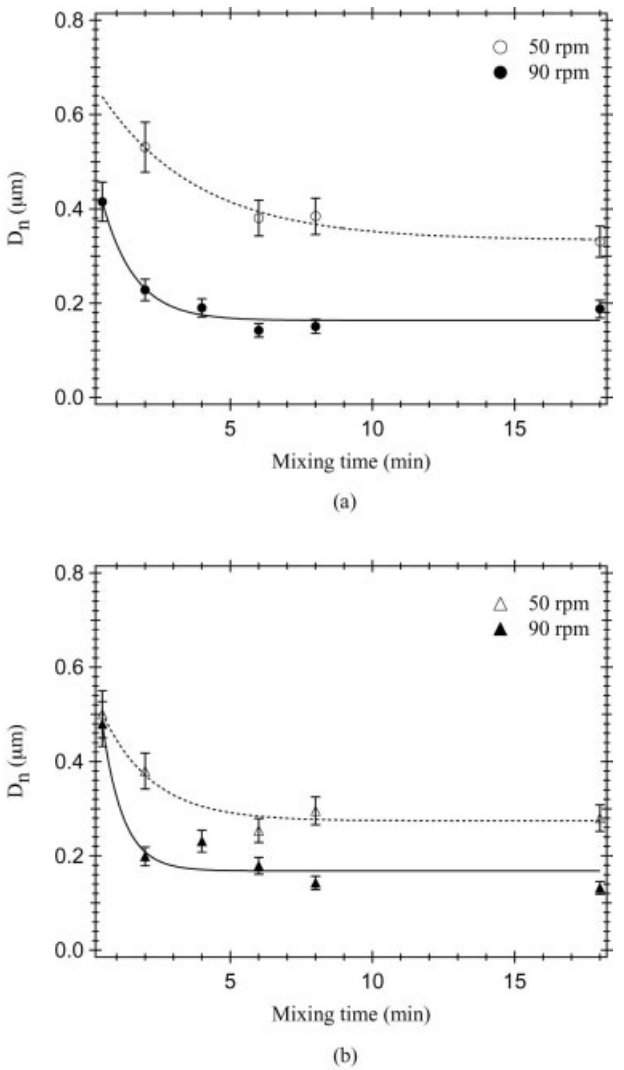

Figure 4 Effect of the screw speed on the evolution of dispersed particle size as a function of mixing time for M-PBT/E–MA–GMA (80/20, w/w) reactive blends at 250°C: (a) pure E–MA–GMA; (b) 48%-modified E–MA–GMA.

Influence of the processing temperature

The effect of the processing temperature on the morphology development at 90 rpm is presented in Figure 8 for M-PBT blends containing virgin E–MA–GMA. Increasing the processing temperature from 250 to 280°C results in a slight increase of the final number-average diameter of the rubber particles from 0.16 to 0.22 μm, respectively. The temperature does not seem to influence the time required for obtaining this final morphology, which is around 2 min in both cases. Table V presents the effect of the processing temperature on the amount of free rubber and of grafted PBT after 8 min of mixing at 90 rpm. As the temperature is increased from 250 to 280°C, the amounts of grafted PBT ($80 - P$) and of the free rubber R decrease. However, according to the precision of the separation procedure, changes are rather limited. To obtain more insight in the rate of the interfacial reaction, the grafting density $1/A$ was also calculated. According to Table V, $1/A$ increased from 0.34 to 0.55 chain/nm^2 as the temperature increased from 250 to 280°C.

The effect of the processing temperature was also analyzed in case of M-PBT/48%-modified E–MA–GMA (80/20 w/w) blends. Figure 9 presents the evolution of the rubber particle size as a function of the mixing time. Increasing the processing temperature promotes larger rubber particles. The final size of the E–MA–GMA particles increased from 0.18 to 0.35 μm. However, compared to PBT blends containing virgin E–MA–GMA, the effect of the temperature here is more significant. After 30 s at 280°C, the final dispersion is already obtained. Table V shows that the reaction proceeds faster as the temperature is increased from 250 to 280°C, that is, the value of $1/A$ jumps from 0.10 to 0.33 chain/nm^2 after 8 min of mixing.

Effect of the matrix viscosity

To highlight the effect of the matrix viscosity on the morphology development but also on the chemical reactions occurring during melt processing, three different PBTs of different molecular masses were used. The three PBT grades exhibit very similar concentrations in carboxyl chain ends, that is, around 45 μequiv/g (see Table I), so the reactivity toward E–MA–GMA should be similar. For PBT/E–MA (80/20, w/w) nonreactive blends, Figure 10 shows that the highest is the PBT molecular mass, the finest is the dispersion. After 18 min of mixing, the size of the E–MA particles became 1.18, 0.75, and 0.35 μm for blends containing L-PBT, M-PBT,and H-PBT, respectively. It is also important to note that the higher the molecular mass of the PBT matrix, the faster is the morphology development. The time required to obtain a stable morphology decreases from 7 min for L-PBT-based blends to less than 2 min for H-PBT/E–MA blends.

More interesting is the development of the blend morphology as a function of the molecular mass of the PBT matrix for PBT/E–MA–GMA (80/20, w/w) reactive blends (Fig. 11). Similar to the nonreactive blend, the higher the matrix viscosity, the finer is the morphology. However, the three curves exhibit the same trends and the final morphology was reached after 2 min of mixing in all cases. It is important to note that the average particle size of the reactive blends and the nonreactive blends are relatively close to each other after 30 s of mixing (cf. Figs. 10 and 11), especially for blends containing H-PBT.

Different PBT/E–MA–GMA blends corresponding to 30 s and 8 min of mixing were also submitted to the Molau's test. A stable emulsion was obtained

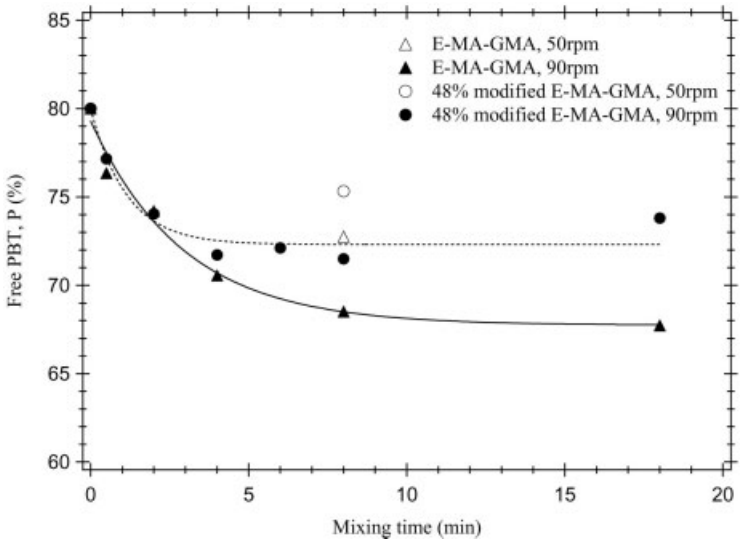

Figure 5 Free PBT concentration after separation for M-PBT/E–MA–GMA (80/20, w/w) reactive blends as a function of mixing time.

for blends processed for 8 min at 250°C, while for blends processed for 30 s, flocculation of the rubber particles in a thin white floating layer was observed. This suggests that stabilization of the rubber particles was not achieved at very short mixing times. To confirm these results, the PBT/E–MA–GMA (80/20, w/w) reactive blends were also characterized using the developed separation procedure (Table VI). Whatever the molecular weight of the PBT matrix, the amount of PBT chains grafted to the rubber particles ($80 - P$) recovered after 30 s of mixing was always lower than 4%, but is not equal to zero. This is in agreement with the fact that smaller dispersed-phase particles were obtained for reactive PBT/E–MA–GMA blends even after 30 s of mixing. Unfortunately, for practical reasons, it was not possible to withdraw samples out of the mixing cavity for mixing times shorter than 30 s. At this stage, it is interesting to focus on the interfacial copolymer concentration (i.e., $1/A$) versus the PBT molecular mass (Table VI). After 30 s of mixing, $1/A$ values were relatively small and lower than 0.05 chains/nm^2. After 8 min of mixing, the interfacial grafting density was rather independent of the PBT molecular mass except for the L-PBT matrix. It is interesting to note that the L-PBT/E–MA–GMA blend exhibits the lowest $1/A$ value after 30 s of mixing and the highest one after 8 min of mixing.

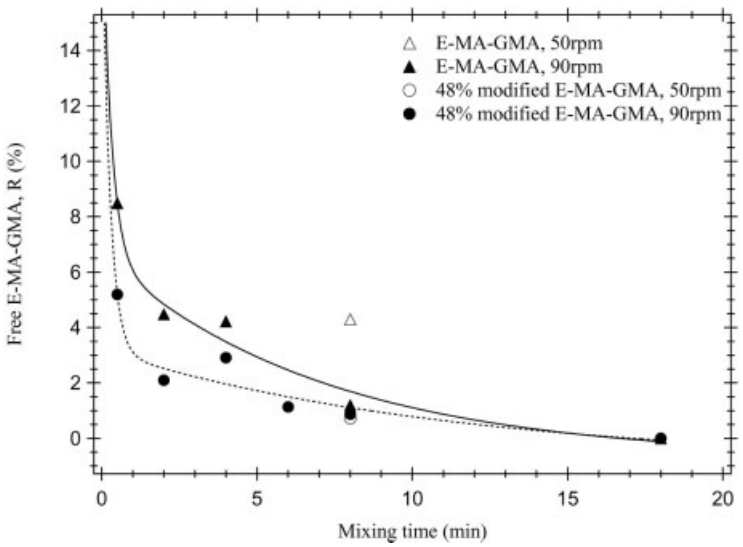

Figure 6 Free E–MA–GMA concentration after separation for M-PBT/E–MA–GMA (80/20, w/w) reactive blends as a function of mixing time.

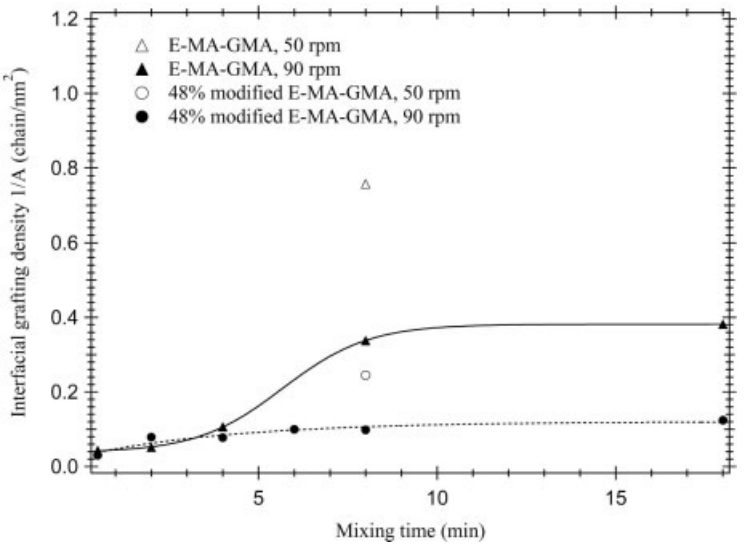

Figure 7 Evolution of the interfacial grafting density for M-PBT/E–MA–GMA (80/20, w/w) reactive blends as a function of the mixing time and of the screw speed.

DISCUSSION

PBT/E–MA nonreactive blends

It is now established that blends of PBT with the E–MA copolymer exhibit the general features of noncompatibilized polymer blends.[22] No trace of a reaction between the PBT chains and the rubber phase was, indeed, obtained using TEM observations and separation experiments. For noncompatibilized polymer blends, the morphology development during processing is determined by the competition between two phenomena: drop breakup and particle coalescence.

According to the theories of Taylor[30] and Wu,[31] the breakup of individual droplets is governed by the ratio of shear to interfacial forces. The first force tends to deform the dispersed-phase particles in the flow field, while the second one tends to maintain them spherically. The predicted particle diameter at equilibrium is given by

$$D = \frac{\sigma_{12}(W_e)_c}{\eta_m \dot{\gamma}} \tag{3}$$

TABLE IV
Interfacial Copolymer Concentration for M-PBT/E–MA–GMA (80/20, w/w) and M-PBT/48%-modified E–MA–GMA (80/20, w/w) Blends After 8 Min of Mixing at 250°C as a Function of Screw Speed

Rubber phase	Screw speed (rpm)	I/A (chain/nm^2)
E–MA–GMA	50	0.77
	90	0.34
48%-modified E–MA–GMA	50	0.24
	90	0.10

where σ_{12} is the interfacial tension (N/m); η_m, the matrix phase viscosity (Pa s); $\dot{\gamma}$, the shear rate (s^{-1}); and $(We)_c$, the critical Weber number, which is a function of the viscosity ratio of the two phases. $(We)_c$ is minimum when the viscosity ratio η_d/η_m is one and is almost invariable for $0.1 < \eta_d/\eta_m < 1$.[32] From eq. (3), it can be concluded that breakup will be favored by an increase of the matrix viscosity or/and of the shear rate. In contrast, an increase of the interfacial tension results in an increase of the particle size.

At relatively high concentrations of the minor component, typically higher than 5 vol %,[33] coalescence of the dispersed-phase particles is no more negligible and must be considered. Particle coarsening caused by coalescence has been extensively studied.[34–44] Coalescence can occur both during flow and quiescent conditions. For two particles to fuse, they must first come into close proximity of each other by some flow process driven by a deformation field, hydrodynamic interaction, gravity, or other forces. Once two particles are in near contact, drainage of the matrix film between the dispersed-phase domains must occur in a relatively short time to allow for particle fusion. The extent of coalescence is a net product of the probability of particle contacts and the probability that any one of those contacts has sufficient matrix film drainage to allow for particle fusion. It is therefore obvious that the extent of coalescence will be intimately related to the blend composition, the matrix viscosity, the phase elasticity, and the shear rate. It increases as the concentration in the dispersed phase increases or/and as the matrix viscosity decreases. The effect of the shear rate is more complex and was recently studied by several authors.[25,37,38] It appeared that the dispersed-phase particle size developed during processing can

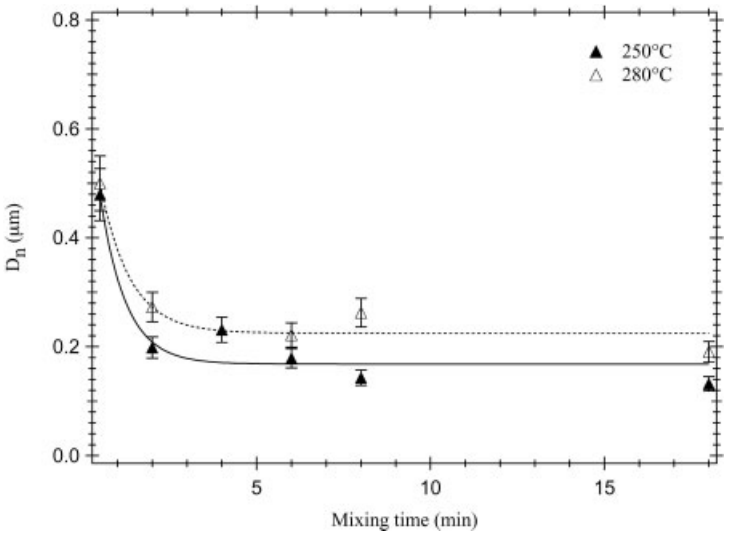

Figure 8 Effect of the processing temperature on the evolution of the particle size as a function of time for M-PBT/E–MA–GMA (80/20, w/w) reactive blends at 90 rpm.

increase, decrease, or show complex nonmonotonic behavior as the shear rate is increased because of the competing effects of increased particle–particle contacts versus decreased contact times. However, according to the most recent studies, it can be concluded that coalescence effects decrease by increasing the shear rate.[45]

Taking into account the competing processes of breakup and coalescence, Fortelny et al.[46] proposed the following equation for the equilibrium particle diameter of the dispersed phase:

$$D_n = \frac{\sigma_{12}(W_e)_c}{\eta_m \dot{\gamma}} + \frac{\sigma_{12}\alpha}{\eta_m f_1}\phi \qquad (4)$$

where Φ is the volume fraction of the dispersed phase; α, the probability of coalescence after collision; and f_1, the slope of the function, $F(W_e)$, describing the frequency of particle breakup at the critical Weber number. In eq. (4), the first term reveals the minimum obtainable particle size according to the classical theory of breakup [cf. eq. (3)], while the second term represents the effects due to coalescence. This equation is very helpful to evaluate the effect of the processing parameters.

Effect of the rotation speed

The average shear rate in an internal mixer is directly related to the rotation speed.[47–49] Using the equation developed by Bousmina et al.,[49] the average shear rate in the internal mixer can be calculated to be 20 and 36 s^{-1} for rotation speeds of 50 and 90 rpm, respectively. Increasing the rotation speed of an internal mixer results, therefore, in an increase of the shear rate in the mixing cavity, which is favorable to drop breakup and unfavorable to coalescence. As a result, the size of the dispersed-phase particles decreases (Fig. 3). The variation of the screw speed also affects the viscosity of the different phases, and in a rigorous approach, such an effect must be evaluated. Assuming that the Cox–Merz law is valid for both the M-PBT homopolymer and E–MA copolymer, the viscosity of the blend components at 250°C can be calculated at 20 and 36 s^{-1} according to Figure 1. In this range of shear rates, the M-PBT viscosity remains almost constant, that is, 276

TABLE V
Amount of Free Rubber *R* and of Grafted PBT and Interfacial Copolymer Concentration for M-PBT/E–MA–GMA (80/20, w/w) Blends After 8 Min of Mixing at 90 rpm as a Function of the Processing Temperature

Rubber phase	Temperature (°C)	Amount of free rubber *R* (%)	Amount of grafted PBT (80 *P*) (%)	$1/A$ (chains/nm^2)
E–MA–GMA	250	1.2	11.5	0.34
	280	0	8.0	0.55
48% modified E–MA–GMA	250	0.8	7.5	0.10
	280	0	5.5	0.33

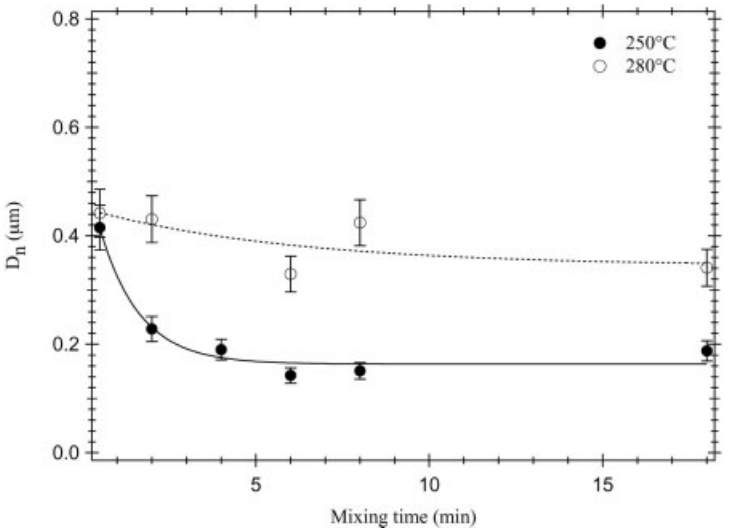

Figure 9 Effect of the processing temperature on the evolution of the particle size as a function of time for M-PBT/48%-modified E–MA–GMA (80/20, w/w) reactive blends at 90 rpm.

and 271 Pa s at 20 and 36 s^{-1}, respectively. In the same time, the viscosity of the E–MA copolymer decreases from 216 to 178 Pa s, respectively, so increasing the shear rate from 20 and 36 s^{-1} results in a slight decrease of the viscosity ratio η_d/η_m from 0.78 to 0.66. In this context, the change in $(We)_c$ can be neglected.

Effect of the PBT viscosity

The effect of the PBT molecular weight on the morphology development (Fig. 10) can also be easily explained according to eq. (4). By increasing the PBT molecular mass, the matrix viscosity is also increased, as revealed in Figures 1 and 2. In this way, the dispersive forces for particle breakup are enhanced, on the one hand, and coalescence is lowered, on the other hand. Increasing the matrix viscosity will also influence the critical Weber number $(We)_c$. At a shear rate of 36 s^{-1}, the viscosity ratio was equal to 0.14 for H-PBT, 0.65 for M-PBT, and 1.25 for L-PBT. In this range of viscosity ratios, the values of $(We)_c$ are not expected to be very different from each other so that this effect can be neglected and, therefore, the formation of larger dispersed particles as the PBT molecular mass is decreased (Fig. 10) is fully explained by the theory.

Additional considerations

As shown in Figures 3 and 10, equilibrium between breakup and coalescence is not instantaneous. At least

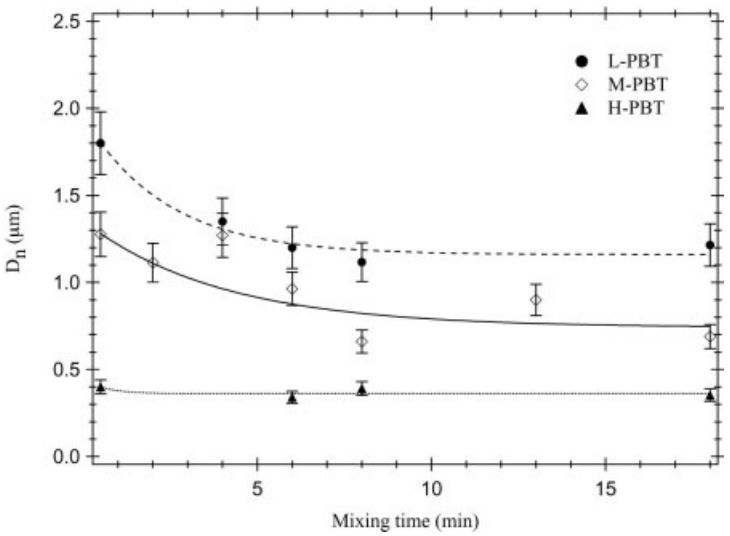

Figure 10 Effect of the matrix viscosity on the evolution of the particle size as a function of time for PBT/E–MA (80/20, w/w) blends at 90 rpm and 250°C.

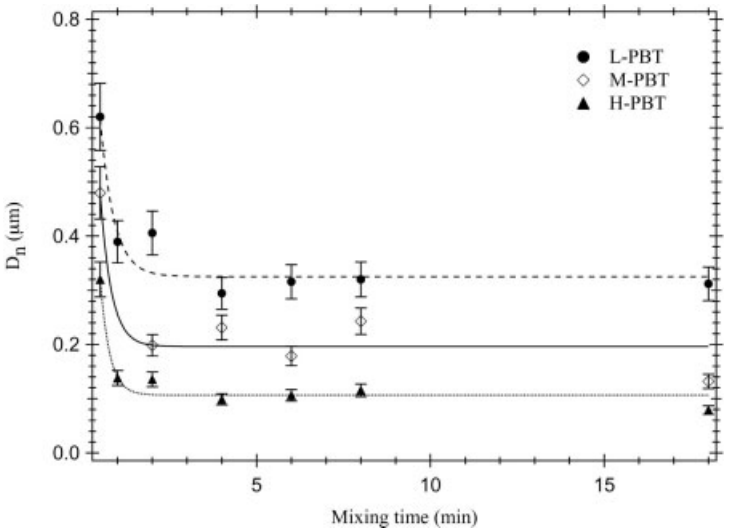

Figure 11 Effect of the matrix viscosity on the evolution of the particle size as a function of time for PBT/E–MA–GMA (80/20, w/w) reactive blends at 90 rpm and 250°C.

4 min of mixing was required to reach the final morphology of the blends, which is quite long for uncompatibilized polymer blends. Similar observations were already made in a previous study[22] and were attributed to the occurrence of reactions between PBT and E–MA at long mixing times. However, such interfacial reactions, if they occur, are too slow and limited to be demonstrated by the characterization techniques used in this work.

PBT/E-MA–GMA reactive blends

In comparison with PBT/E–MA nonreactive blends, PBT blends containing pure or modified E–MA–GMA exhibit, in all cases, a finer morphology. This results from the formation of the E–MA–GMA/PBT graft copolymers at the blend interface due to the reaction between the PBT carboxyl end groups and the rubber epoxide functions during processing.[22] It is now well established that formation of a compatibilizer at the interface will influence, to a large extent, the processes of breakup and coalescence discussed above. It is responsible for the significant stretching of the dispersed phase into a very fine fiber before the interfacial instabilities become important and lead to fiber breakup.[25,35] In the same way, the steric and entropic barrier formed by the compatibilizer at the interface and the loss of mobility of the interface result in strong retardation if not inhibition of the coalescence. As a result, the size of the dispersed-phase particles decreases to a large extent.

To explain the results, the relative kinetics of both physical and chemical processes has to be considered. As explained elsewhere,[22] PBT/E–MA–GMA blends exhibit a very complex behavior. Two competitive reactions take place during melt processing, namely, (1) blend compatibilization and (2) rapid crosslinking of the rubber phase. According to several authors,[26,50,51] the reaction between epoxide functions and carboxyl groups is expected to be quite slow. In this context, we postulate that the morphology development can be subdivided in two successive steps (Scheme 1). In the early stages of the mixing, that is, at very short mixing times, the blend morphology is essentially governed by physical factors such as the viscosity of both phases, the blend composition, the shear rate, and the interfacial tension. This is the "physics-controlled" regime (Zone I in Scheme 1). Within this period of time, the evolution of the blend morphology should be similar to that of the uncom-

TABLE VI
Amount of Grafted PBT (80 − *P*) and of Free E-MA-GMA (*R*) Recovered After Separation for PBT/E–MA–GMA (80/20, w/w) Blends and Interfacial Copolymer Coverage (1/*A*) as a Function of the PBT Molecular Weight

	30 s of mixing			8 min of mixing		
PBT grade	$80-P$ (%)	R (%)	$1/A$ (chain/nm^2)	$80-P$ (%)	R (%)	$1/A$ (chain/nm^2)
L-PBT	1.7	11.6	0.013	6.1	2.3	0.52
M-PBT	3.1	8.5	0.04	11.5	1.2	0.34
H-PBT	3.2	8.0	0.05	26.8	0.15	0.38

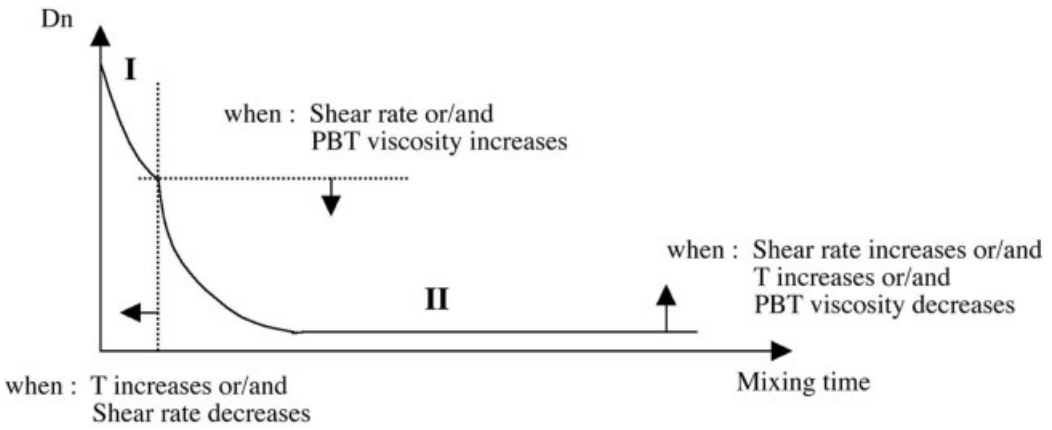

Scheme 1 Schematic representation of the mixing process. I: "physics-controlled" regime; II: "chemistry-controlled" regime. As schematically presented, the transition between the two regimes is dependent on the processing conditions.

patibilized blends and should then be governed by eq. (4). As the mixing time increases, the chemical reactions take place progressively, leading to a further refinement of the morphology and its subsequent stabilization (Zone II in Scheme 1). In other words, the system shifts from a "physics-controlled" to a "chemistry-controlled" regime. In this latter step, the evolution of the particle size is governed by the relative kinetics between the compatibilization reaction and the crosslinking of the rubber phase. The transition between the two regimes is not sharp but rather diffuse. It is intimately related to the kinetics of the chemical reactions and to the processing conditions. Scheme 1 is very useful to explain the experimental observations.

Effect of the rotation speed

As already explained for M-PBT/E–MA nonreactive blends, increasing the screw speed results, essentially, in a finer dispersion of the minor phase in the early stages of the mixing and, therefore, in a larger interfacial area. So, the rate of the interfacial reaction is enhanced, and as a result, the rubber particles are rapidly stabilized against coalescence and further dispersed [see Fig. 4(a,4b)]. The effect of the crosslinking reaction has also to be taken into account. In the case of M-PBT blends containing pure E–MA–GMA, the occurrence of this reaction is somewhat delayed so that it becomes significant after complete dispersion of the rubber phase. In the case of M-PBT/48%-modified E–MA–GMA blends, the rubber crosslinking occurs immediately in the melt, due to the presence of the secondary hydroxyl functions on the rubber chains from the beginning of the mixing.[23] The dispersed-phase particles become directly more viscous and more elastic, which is unfavorable to breakup. It is worth noting that rubber crosslinking is also expected to hinder the process of coalescence. All these observations explain why the effect of the screw speed is more pronounced for blends containing 48%-modified E–MA–GMA [see Fig. 4(a,b)].

It is interesting to note that at high shear rate, that is, 36 s^{-1}, M-PBT/E–MA–GMA and M-PBT/48%-modified E–MA–GMA exhibit the same morphology development despite the fact that the crosslinking reaction proceeds in a very different way. We assume that, at a sufficiently high shear rate, the physical processes of dispersion and coalescence can, over a longer period of time, overcome the effects due to the chemical reactions. In other words, the dispersive forces are so important that the difference in the rubber crosslinking density existing in the early stages of the mixing does not modify the rubber-phase dispersion. Very small particles are then generated and rapidly stabilized through interfacial coupling between PBT and E–MA–GMA. It is worth noting that even if both systems exhibit the same morphology when processed at 90 rpm the elastic properties of the dispersed-phase particles, and, therefore, the ultimate blend properties, are expected to be very different from one system to the other.[23]

For M-PBT blends containing 48%-modified E–MA–GMA, the average area occupied by the PBT grafts at the interface was larger, but also reached a constant value more rapidly whatever the rotation speed (Fig. 7). This results from the smaller initial amount of epoxide groups compared to virgin E–MA–GMA. Moreover, these groups are rapidly consumed through the crosslinking reaction, which takes place immediately in the melt. In contrast, since the area available for the interfacial coupling reaction is directly proportional to the rotation speed, it is surprising to note that, whatever the used rubber phase, $1/A$ decreases with the rotation speed (Table IV). The only way to explain this apparent contradiction is to consider the crosslinking of the rubber phase. From geometrical considerations, one can assume that the

smaller the dispersed-phase particles, the faster is the consumption of available epoxide groups due to crosslinking. So, epoxide groups available for interfacial reaction vanish rapidly as the mixing time increases. Such an effect is expected to be more pronounced at high shear rates due to the finer dispersion of the rubber phase. At low shear rates, the interfacial reaction can then proceed further due to a higher initial concentration of epoxide groups per particle and to their slower consumption by the crosslinking reaction. It is worth noting that the rapid consumption of the epoxide groups is favored by the fact that the crosslinking of the rubber particles not only consumes the epoxide functionalities but also hinders the coalescence phenomena.

Effect of the processing temperature

The processing temperature is expected to influence both the physical processes of dispersion as well as the chemical reactions. On the one hand, the increase of the temperature from 250 to 280°C leads to the lowering of the phase viscosities as demonstrated in Figures 1 and 2. The viscosity ratio η_d/η_m between E–MA–GMA and PBT at a shear rate of 36 s^{-1} increases slightly from 0.83 to 1.02 at 250 and 280°C, respectively. According to the equation of Fortelny et al.[46] [eq. (4)], the dispersive forces for particle breakup are, consequently, lowered, on the one hand, and coalescence is enhanced, on the other hand, due to an enhanced drainage of the matrix film. This supports the formation of larger dispersed-phase particles by increasing the processing temperature at the early stages of the mixing.

On the other hand, as the temperature is increased, both interfacial coupling and rubber crosslinking are expected to proceed faster. In other words, the transition from the "physics-controlled" regime to the "chemistry-controlled" regime is shifted to shorter mixing times. This is confirmed in Table V. As the temperature was increased from 250 to 280°C, the amount of free rubber chains decreased and the interfacial copolymer concentration increased. The faster compatibilization is favorable to the rubber dispersion, while the faster rubber crosslinking leads to an increase of the rubber- phase elasticity, which is nonfavorable to drop breakup and coalescence. The coarser morphology obtained at 280°C appears, therefore, to result from two opposite phenomena: (i) coarsening of the rubber domains due to lowered breakup, enhanced coalescence, and faster crosslinking and (ii) faster compatibilization. For M-PBT49 blends containing pure E–MA–GMA, the effect of the rubber crosslinking is limited, since this reaction proceeds consecutively after the compatibilization reaction. For M-PBT49/48%-modified E–MA–GMA blends, competition between the compatibilization and the crosslinking reactions takes place immediately in the melt. According to Figure 9, it is clear that, at 280°C, the rate of the crosslinking reaction is so high that it overcomes the effect due to the physical dispersion and to the interfacial reaction, that is, blend compatibilization. As a result, large dispersed-phase particles of approximately 0.35 μm are formed. In the previous section, the possibility to favor physical processes in regard to the chemical reactions was envisioned. Here, we demonstrated that, even at high shear rates, the effect of chemical reactions can be highlighted by an adequate adjustment of the processing temperature.

Effect of the matrix viscosity

In Figure 11, it appears clearly that the matrix viscosity has an important influence on the final blend morphology. The higher the PBT molecular weight, the finer is the morphology. Such results are in agreement with those obtained by Hale et al.[52] for PBT/ABS blends compatibilized by methyl methacrylate–glycidyl methacrylate–ethyl acrylate terpolymers. However, they are in contradiction with the study by Dedecker and Groeninckx[53] on PA-6/(PMMA/SMA) blends. In this latter case, the authors found that, in contrast to noncompatibilized PA-6/PMMA blends, no influence of the PA-6 molecular weight on the final blend morphology was found when 5 wt % of a styrene–cyclic anhydride copolymer (SMA) was used. Once again, the kinetics of interfacial coupling has to be considered. In case of amine/cyclic anhydride functionalities, the interfacial reaction is very fast and proceeds mainly during the initial softening/melting step of the blending. The interface is covered as fast as it is generated. Compared to the coupling reaction between primary amine and cyclic anhydride, the reaction between epoxide groups and carboxyl PBT chain ends is expected to proceed slowly. In the present cases, we assume that, in the early stages of the mixing, the morphology is governed by the physical processes of breakup and coalescence (Scheme 1). Such a hypothesis is also confirmed by the fact that PBT/E–MA nonreactive blends and PBT/E–MA–GMA reactive blends exhibit similar morphologies at very short mixing times (Figs. 10 and 11). Progressively, the chemical reactions, that is, compatibilization and crosslinking reactions, develop, leading to further reduction in the size of the dispersed-phase particles and to interface stabilization. As the different PBT grades exhibit a very close concentration in carboxyl chain ends, the chemistry-induced reduction in the rubber particle size is similar in the three cases (Fig. 11). Indeed, the time required for reaching the final morphology is the same whatever the PBT molecular weight, which is not the case for PBT/E–MA nonreactive blends.

In Table VI, we mentioned that the copolymer interfacial coverage, $1/A$, is rather independent of the PBT molecular mass except for the L-PBT45 matrix. The L-PBT45/E–MA–GMA blend exhibits the lowest $1/A$ value after 30 s of mixing and the highest one after 8 min of mixing. Since diffusion effects are expected to be rather limited in the case of a slow interfacial reaction,[54] such a surprising result should be related to the crosslinking of the rubber phase. From geometrical considerations, one can assume that the smaller are the dispersed-phase particles (and then the higher the PBT molecular mass), the faster is the consumption of available epoxide groups due to crosslinking. Such an assumption is supported by the fact that the amount of free rubber R recovered after 8 min of mixing decreases as the PBT molecular mass is increased (Table VI). So, the epoxide groups are expected to vanish more rapidly in case of PBT with the higher molecular mass. Moreover, as the rubber phase crosslinks, the diffusion of the epoxide groups toward the interface is largely hindered. At long mixing times, no epoxide groups are available for further interfacial reactions. In contrast, for blends containing L-PBT45, the grafting of the PBT chains can proceed further due to the higher amount of available epoxide groups per dispersed-phase particles. This results in a slightly larger interfacial copolymer concentration.

CONCLUSIONS

The influence of the processing parameters, such as the mixing efficiency, the processing temperature, and the matrix viscosity, on the morphology of PBT/E–MA and PBT/E–MA–GMA polymer blends was investigated. The morphology development can be divided in two successive regimes: In the early stages of the mixing processes, the particle size is essentially influenced by the physical dispersion processes, that is, breakup and coalescence. In this regime, the higher the matrix viscosity or/and the shear rate, the finer is the morphology. As the mixing time is increased, the effects of the chemical reactions become more and more significant and the system shifts from a "physics-controlled" regime to a "chemistry-controlled" regime. Further decrease in the particle size is obtained as a result of the blend compatibilization and the inhibition of the coalescence phenomena. The shift between the two regimes is progressive and is intimately related to the processing conditions. Hence, the effect of the chemical reactions, that is, interfacial grafting and rubber crosslinking, is highlighted by increasing the temperature and/or decreasing the shear rate.

In the case of PBT/E–MA nonreactive blends, the "chemistry-controlled" regime is not present so that the morphology development is in good agreement with the classical theories of particle breakup and coalescence. In the case of PBT/E–MA–GMA reactive blends, the morphology development was seen to be more complex and intimately related to the relative kinetics between the physical dispersion processes and the chemical reactions. By an adequate choice of the processing conditions, it is possible to favor the occurrence of one phenomenon with respect to the other. The extent of PBT grafting is intimately related to the PBT molecular mass and to the size of the dispersed-phase particles. The highest interfacial copolymer coverage is obtained for the largest rubber particles due to a slower consumption of the available epoxide groups by the crosslinking reaction.

One of the authors (P. M.) would like to thank DSM n.v. for both financial and technical support.

References

1. Bottenbruch, L. Engineering Thermoplastics: Polycarbonates, Polyacetals, Polyesters, Cellulose Esters; Hanser: New York, 1998.
2. Gravalos, K. G.; Kallitsis, J. K.; Kalfoglou, N. K. Polymer 1995, 36, 1393.
3. Porter, R. S.; Wang, L. H. Polymer 1992, 33, 2019.
4. Legros, A.; Carreau, P .J.; Favis, B. D.; Michel, A. Polymer 1994, 35, 758.
5. Carté, T. L.; Moet, A. J Appl Polym Sci 1993, 48, 611.
6. Cecere, A.; Greco, R.; Ragosta, G.; Scarinzi, G.; Taglialatela, A. Polymer 1990, 31, 1239.
7. Akkapeddi, M. K.; Van Buskirk, B.; Mason, C. D.; Chung, S. S.; Swamikannu, X. Polym Eng Sci 1995, 35, 72.
8. Sun, Y. J.; Hu, G. H.; Lambla, M.; Kotlar, H. K. Polymer 1996, 37, 4119.
9. Hu, G. H.; Sun, Y. J.; Lambla, M. Polym Eng Sci 1996, 36, 676.
10. Tsai, C. H.; Chan, F. C. J Appl Polym Sci 1996, 61, 321.
11. Wang, X. H.; Zhang, H. X.; Wang, Z. G.; Jiang, B. Z. Polymer 1997, 38, 1569.
12. Hale, W.; Keskkula, H.; Paul, D. R. Polymer 1999, 40, 365.
13. Van Duin, M.; Neilen, M. G. M., to be submitted for publication in J Appl Polym Sci.
14. Hert, M. Angew Makromol Chem 1992, 196, 89.
15. Penco, M.; Pastorino, M. A.; Occhiello, E.; Garbassi, F.; Braglia, R.; Giannotta, G. J Appl Polym Sci 1995, 57, 329.
16. Dagli, S. S.; Kamdar, K. M. Polym Eng Sci 1994, 34, 1709.
17. Heino, M.; Kirjava, J.; Hietaoja, P.; Seppälä, J. J Appl Polym Sci 1997, 65, 241.
18. Kalfoglou, N. K.; Skafidas, D. S.; Kallitsis, J. K.; Lambert, J. C.; Van der Stappen, L. Polymer 1995, 36, 4453.
19. Pesneau, I.; Llauro, M. F.; Grégoire, M.; Michel, A. J Appl Polym Sci 1997, 65, 2457.
20. Vainio, T.; Hu, G. H.; Lambla, M.; Seppälä, J. J Appl Polym Sci 1997, 63, 883.
21. Brady, A. J.; Keskkula, H.; Paul, D. R. Polymer 1994, 35, 3665.
22. Martin, P.; Devaux, J.; Legras, R.; van Gurp, M.; van Duin, M. Polymer 2001, 42, 2463.
23. Martin, P. Ph.D. Thesis, Univ. Catholique de Louvain, Belgium, 2002.
24. Papke, N.; Karger-Kocsis, J. J Appl Polym Sci 1999, 74, 2616.
25. Fortelny, I.; Zivny, A. Polym Eng Sci 1995, 35, 1872.
26. Liu, N. C.; Baker, W. E. Adv Polym Tech 1992, 11, 249.
27. Kim, J. K.; Kim, S.; Park, C. E. Polymer 1997, 38, 2155.
28. Paul, D. R.; Newman, S. Polymer Blends; Academic: New York, 1976; Vol. 2.

29. Pagnoulle, C. Ph.D. Thesis, Université de Liège, Belgium, 2000.
30. Taylor, G. I. Proc R Soc A 1934, 146, 501.
31. Wu, S. Polym Eng Sci 1987, 27, 335.
32. Grace, H. P. Chem Eng Commun 1982, 14, 225.
33. Favis, B. D. In Polymer Blends, Vol. 1: Formulations; Paul, D. R.; Bucknall, C. B., Eds.: Wiley: New York, 1999; Chapter 16.
34. Cheng, T. W.; Keskkula, H.; Paul D. R. J Appl Polym Sci 1992, 45, 1245.
35. Kelnar, I.; Fortelny, I. J Polym Eng 1995, 14, 269.
36. Majumbar, B.; Paul, D. R.; Oshinski, A. J. Polymer 1997, 38, 1787.
37. Sundararaj, U.; Macosko, C. W. Macromolecules 1995, 28, 2647.
38. Fortelny, I.; Zivny, A. Polymer 1995, 36, 4113.
39. Elmendorp, J. J.; van der Vegt, A. K. In Two-phase Polymer Systems; Utracki, L. A., Ed.; Carl Hanser: Munich, 1991; Chapter 6.
40. Sondergaard, K.; Lyngaae-Jorgensen, J. In Flow-induced Structure in Polymers; Nakatani, A. I.; Dadmund, M. D., Eds.; American Chemical Society: Washington, DC, 1995; Chapter 12.
41. Favis, B. D.; Willis, J. M. J Polym Sci Part B Polym Phys 1990, 28, 2259.
42. Fortelny, I.; Kovar, J.; Stephan, M. J. Elast Plast 1996, 28, 106.
43. Janssen, J. M. H.; Meijer, H. E. H. Polym Eng Sci 1987, 35, 1766.
44. Elmendorp, J. J.; van der Vegt, A. K. Polym Eng Sci 1986, 26, 1332.
45. Lyu, S. P.; Bates, F. S.; Macosko, C. W. AlChE J 2002, 48, 7.
46. Fortelny, I.; Cerna, Z.; Binho, J.; Kovar, J. J Appl Polym Sci 1993, 48, 1731.
47. Wood, F. W.; Goff, T. C. Engl Staerke 1973, 25, 89.
48. Aerts, L.; Verspaille, M. Starch/Staerke 2001, 53, 59.
49. Bousmina, M.; Ait-Kadi, A.; Faisant, J. B. J Rheol 1999, 43, 415.
50. Majumbar, B.; Paul, D. R. In Polymer Blends, Vol. 1: Formulations; Paul, D. R.; Bucknall, C. B., Eds.; Wiley: New York, 1999; Chapter 17.
51. Cigana, P.; Favis, B. D. Polym Mater Sci Eng 1995, 73, 16.
52. Hale, W.; Lee, J.-H.; Keskkula, H.; Paul, D. R. Polymer 1999, 40, 3621.
53. Dedecker, K.; Groeninckx, G. Polymer 1998, 39, 4985.
54. Fallais, I. Ph.D. Thesis, Université Catholique de Louvain, Belgium, 2001.